LANDTECHNIK
AGRICULTURAL ENGINEERING

Net traction force/slip behaviour of tractor tyres - practical oriented measurement and simulation with the Hohenheim Machine Model

Arwid Meiners, Stefan Böttinger, Nicolò Regazzi

Within investigations on the fuel consumption of agricultural process chains, a simulation model for tractors is being developed which enables the calculation of time-related fuel consumption of static operating points. The transmission of forces between tyre and soil in longitudinal direction is mapped by a regression model, which however is based on outdated data. The current status of tyre size and technology can thus only be simulated inadequately. Based on the development and discussion of a suitable measurement methodology to determine the net traction force/slip-curves of modern tyres of larger dimensions, measurements with different tyre sizes are carried out and the results are presented. The introduction of correction factors in the empirical regression equations opens a way to update the tyre-soil model, which is done on the basis of the measured curves. Investigations on the influence of different parameters on the traction behaviour of standard tractors up to 300 kW nominal power are possible with the updated model and are presented as results.

Key words
Efficiency, simulation, tractor tyres, tyre-soil interaction

Over the past few years, the discussion on emissions of climate-relevant gases has shaped political decisions within the EU by defining climate protection targets and successively tightening limit values (EUROPÄISCHER RAT 2014, EUROPÄISCHE KOMMISSION 2014). The objectives for Germany envisage a 34% reduction in greenhouse gas emissions for the agricultural sector by 2030 compared with 1990 levels (BUNDESMINISTERIUM FÜR UMWELT, NATURSCHUTZ, BAU UND REAKTORSICHERHEIT 2018). The agricultural machinery sector is not explicitly highlighted here. Following the introduction and amendment of legally prescribed limit values for CO_2 emissions from passenger cars (EUROPÄISCHES PARLAMENT UND RAT DER EUROPÄISCHEN UNION 2009, 2014), a similar procedure could also be applied to agricultural machinery. As an alternative, the holistic approach of a voluntary self-commitment of the agricultural machinery industry to reduce CO_2 emissions presented by FLECK et al. (2014) can be seen in relation to legislation. Within the joint research project EcoTech (Efficient fuel use in Agricultural Technology), first steps are being developed along this path (DECKER and FRERICHS 2017). The focus is on the calculation of the development of fuel consumption on virtual model farms from the reference year 1990, over 2016 as the current status at the beginning of the research project, to the year 2030. It is shown what potential the developments in agricultural engineering already have on the fuel consumption of a farm and how this will continue in the future.

The development of a simulation model makes it possible to calculate fuel consumption in agricultural process chains, which is essential especially with regard to future developments. Within the consortium the Institute of Agricultural Engineering at the University of Hohenheim is responsible for the calculation of time-related fuel consumption of agricultural machinery in l/h due to the development of the Hohenheim Machine Model (HMM) during the project (Meiners and Böttinger 2018).

The modular model design takes machine combinations of one machine with one or more front and rear implements into account. In principle, it is possible to combine any combination of machines and implements within the context of a real, reasonable assignment of machine and implement. This can be a tractor with front weight and disc harrow or a combine harvester with grain header. The implements deliver forces, torques or powers from different calculation approaches, which are transmitted to the machine. In the component-based modelling approach, these are transferred by stored transmission ratios and efficiency factors or characteristic maps from the tyre via the drive train to the engine and result in a fuel consumption corresponding to the load point of the engine (Meiners et al. 2017). Static operating points for the different part times are simulated according to the KTBL scheme of time structuring (Winkler and Frisch 2014). Within the simulation model, the modelling of the complex contact between tyre and ground for transferring forces in longitudinal direction is based on the tyre-soil model developed by Schreiber (2006). This regression model is based on the approach that the slip-dependent curves for rolling resistance ratio ρ and net traction ratio κ can be described and mathematically mapped using the four characteristic parameters $-\rho_e$, $\kappa`(\sigma = 0)$, $\sigma_{\kappa,max}$ and κ_{max} shown in Figure 1.
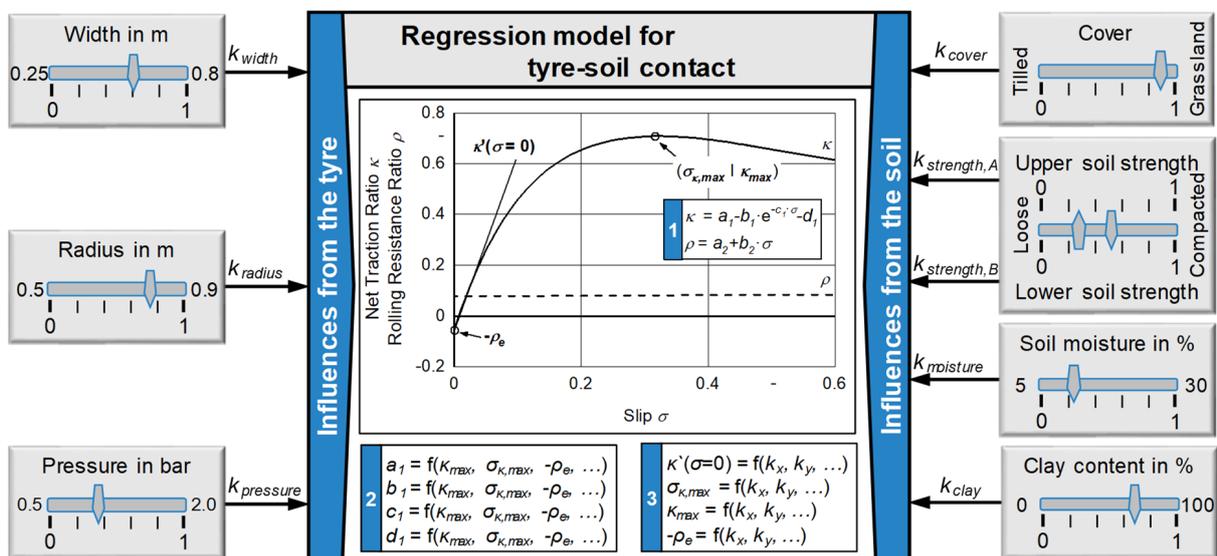

Figure 1: Regression model for the tyre-soil contact

The coefficients $a_1 - d_1$ and $a_2 - b_2$ of Equations 1 and 2 can be expressed as a function of these characteristic parameters using the calculation method shown by SCHREIBER and KUTZBACH (2008).

$$\kappa = a_1 - b_1 \cdot e^{-c_1 \cdot \sigma} - d_1 \cdot \sigma \qquad \text{(Eq. 1)}$$

$$\rho = a_2 + b_2 \cdot \sigma \qquad \text{(Eq. 2)}$$

The empirical Equations 3–5, which are based on an extensive data basis of measured net traction ratio/slip and rolling resistance ratio/slip curves of STEINKAMPF (1986), provide a correlation between the most significant influencing variables on the part of the tyre and the ground on the traction behaviour and therefore on the values of the characteristic parameters.

$$\kappa_{max} = 0.31 + 0.13 k_{cover} + 0.11 k_{strength,A} + 0.09 k_{strength,B} + 0.07 k_{clay} \qquad \text{(Eq. 3)}$$

$$+0.09(-4k_{moisture}^2 + 4k_{moisture}) + 0.13 k_{tyre}$$

$$\sigma_{\kappa,max} = \frac{55 - 18k_{cover} - 12k_{strength,A} - 8k_{strength,B} - 6k_{clay} + 8k_{moisture}}{100} \qquad \text{(Eq. 4)}$$

$$\kappa'(0) = 5 + 2{,}8 k_{cover} + 1{,}3 k_{strength,A} \qquad \text{(Eq. 5)}$$

Since the net traction force is to be in the foreground, the parameter $-\rho_e$ is not considered any further (SCHREIBER 2006). As regression coefficients, the k-factors describe the respective factor in its characteristic between minimum and maximum value occurring in the database. For a more practical application, the absolute values shown in Figure 1 are converted into relative values ranging from 0 to 1. In the case of vegetation (k_{cover}) and soil strength for upper ($k_{strength,A}$) and lower soil layer ($k_{strength,B}$), the characteristics are of a rather qualitative nature depending on the soil condition, for example the cultivation (e.g. tilled). The soil type can be varied via k_{clay} between the two extreme forms pure sand and clay soil. The influences of the tyre are summarized in the factor k_{tyre} as an abstract equivalent of the contact patch formed by the tyre width (0.25–0.8 m), the rolling radius (0.5–0.9 m) and the tyre inflation pressure (0.5–2.0 bar)(SCHREIBER 2006).

The underlying database was created with tyre technologies from the 1980s and therefore takes tyres up to a maximum size of 20.8 R 38 into account. The possibilities for modelling modern tractor tyres are therefore limited in terms of technology and dimension. The latter can in principle be compensated by extrapolating the regression equations beyond the valid range. The validity of the results is to be tested, especially with regard to developments in tyre design (from bias-ply to radial) and materials since then, and nevertheless needs to be proven in general. The orientation on performance classes defined by the KTBL (KTBL 2016) when simulating with the HMM leads to a fixed allocation of tyre sizes for standard tractors. Table 1 shows the sizes on the rear axle that are outside the previous validity range of the tyre-soil model. The net traction force/slip behaviour of these tyres must be investigated using a suitable measurement methodology and compared to the results of the tyre-soil model. Hence, the following investigation will focus on the influences of the tyre.

Table 1: Tyre dimensions outside the validity range of the tyre-soil model, based on KTBL (2016)

Performance class standard tractor	Tyre size rear axle
75–92 kW	520/70 R 38
93–111 kW	600/65 R 38
112–147 kW	650/65 R 38
148–184 kW	650/65 R 42
185–215 kW	710/70 R 42
216–250 kW	710/75 R 42
251–300 kW	710/75 R 42

Development and discussion of the measurement methodology

The measurement of net traction ratio/slip curves with a single wheel tester, as it is available at the institute (ARMBRUSTER 1991), offers the advantage of an isolated examination of the individual tyre and the targeted influence on boundary conditions, such as wheel load. Due to the complex technology, however, the test application proves to be not flexible enough and therefore not suitable for practical use. The tyres to be tested must be available individually and the use of standard rims for mounting the tyre on the measuring hub of the test equipment is not possible. Special rims are required for each tyre size. There are restrictions with regard to tyre dimensions and wheel load, which is why the investigation required here, cannot be realized with this method. Measurements using the whole vehicle, whereby the tractor can only be seen as the carrier vehicle of the tyre to be tested, allow for more flexible operating conditions. According to the measurement methodology discussed by Zoz and GRISSO (2003) and applied by SCHULZE ZUMKLEY (2017), besides a proper measurement for drawbar pull, only an additional braking vehicle is required. However, the measurement of drawbar pull leads to a degree of uncertainty, as the driven rear axle cannot be examined separately from the pushed front axle. An extrapolation to the net traction force is not possible without further ado. In addition to prove the practicality of the measurement methodology, the first step will therefore be to investigate the relationship between the forces acting on the driven wheel and those acting on the whole vehicle.

The Fendt 313 Vario tractor available at the institute is used as measuring vehicle. Measuring rims on both rear wheels (520/70 R 38) and one front wheel (480/70 R 24) measure the forces acting on the tyre in the three spatial directions (BÜRGER and BÖTTINGER 2017). A three-axis dynamometer in the rear three-point hitch measures the forces induced into the vehicle. Six load cells, three in x-, one in y- and two in z-direction with a measuring range of up to 100 kN each (accuracy class 0.1), are installed. The test setup is shown in Figure 2. The braking vehicle coupled via a tow bar, which is not shown here, applies the forces. The rigid connection allows drawbar pull and compressive forces to be induced. In addition to the forces acting on the whole vehicle in the test, Figure 2 (right) shows the rear axle with the resulting forces and the drive torque cut free. The total net traction force $F_{NT,RA}$ of the two rear wheels is given by Equation 6.

$$F_{NT,RA} = F_{DP,x} + F_{P,FA} \qquad\qquad\qquad\qquad\qquad\qquad\qquad\qquad\text{(Eq. 6)}$$
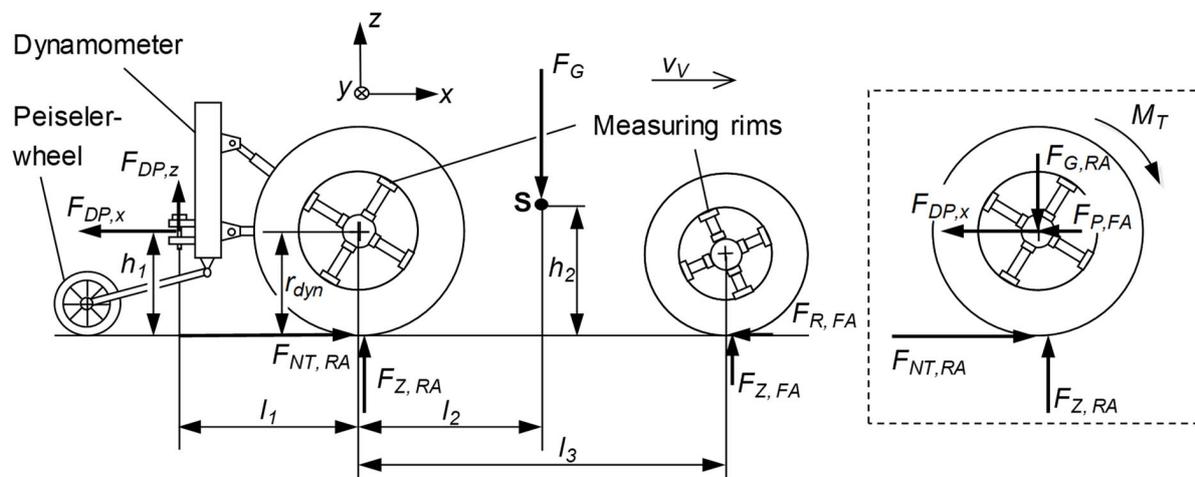
Figure 2: Test setup (left) and resulting forces at the rear wheels (right)

The measurement of the characteristic curve for a test configuration is carried out continuously. The relevant slip range is completely covered within one measurement. The measuring vehicle travels at a velocity of $v_{v,theor}$ = const. = 3 km/h, which is adjusted by the cruise control and kept constant during the entire test. The four-wheel drive is off, the rear axle differential is engaged and the engine is at maximum speed. At the beginning of the test, the braking vehicle pushes to generate a negative slip before the speed of the braking vehicle is steadily reduced. A change of direction of the induced force occurs followed by an increase of force and slip on the measuring vehicle. The static wheel load shift causes additional load to be transferred from the front axle to the rear axle as the drawbar pull increases. All tests are carried out in a specially prepared soil bin, which consists of the soil type silty loam (uL). In preparation to each test, the soil is harrowed at about 12 cm using a rotary harrow to ensure that the initial conditions remain constant. The soil moisture can be described as dry, from a qualitative point of view.

Figure 3 shows the time based course of a complete measurement for a tyre inflation pressure of p = 1.6 bar. The measured drawbar pull is already added to the rolling resistance force $F_{R,FA}$ determined at the front axle and is referred to as $F_{NT,RA,calc}$. In addition to the measured values for the sum of the net traction forces on both rear wheels $F_{NT,RA}$ and axle load $F_{G,RA}$, the curve of a calculated axle load on the rear axle $F_{G,RA,calc}$ is also shown. This results from a static balance of forces on the measuring vehicle taking into account the geometric relations from Figure 2, the axle load distribution measured on wheel load scales before the test and the time varying drawbar pull. The relevant radius on the wheel is the dynamic rolling radius r_{dyn} according to the tyre manufacturer's specifications. Wheel load, internal tyre pressure and ground conditions have an influence on the effective radius, in some cases even inverse, but according to KUTZBACH et al. (2019) the error is often small. For a tyre 710/75 R 42 (SCHULZE ZUMKLEY 2017), for example, determined a reduction of the rolling radius by 2 % for a doubling of the wheel load, whereas an increase of the tyre inflation pressure from 0.9 to 2.1 bar increases the rolling radius by 1.5 %. Vertical forces in the z-direction caused by the measuring vehicle digging into the soil with higher slip are measured with the dynamometer and taken into account in the calculation.
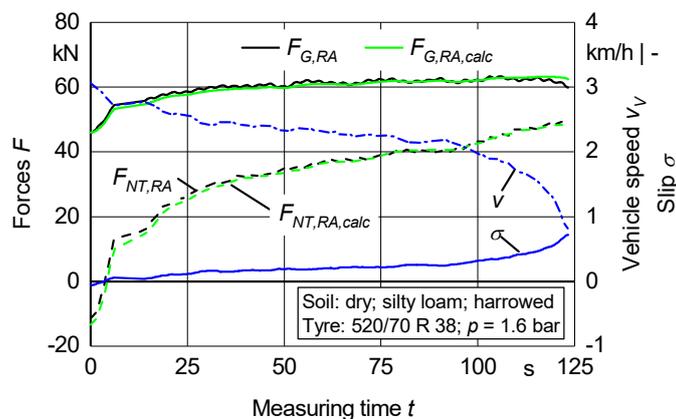
Figure 3: Measured forces, slip and velocity for one test procedure

The effective velocity v_V is measured using a Peiseler wheel attached to the dynamometer. Slip σ and net traction ratio κ are generally calculated according to Equations 7 and 8. The switch from pushing to pulling enables the smooth transition from negative to positive slip at t = 5 s to be fully mapped. The net traction force reaches the maximum of the measurement at approximately 60 % slip with $F_{NT,RA}$ = 49 kN. Higher slip values are not provoked because they are outside the range of practical relevance. The net traction forces and axle loads of the rear axle measured directly with the measuring rims ($F_{NT,RA}$ and $F_{G,RA}$) and indirectly with the dynamometer ($F_{NT,RA,calc}$ and $F_{G,RA,calc}$) show good correlation within the entire measuring range.

$$\sigma = \frac{v_{F,theor} - v_F}{v_{F,theor}} \qquad\qquad \text{(Eq. 7)}$$

$$\kappa = \frac{F_T}{F_Z} \qquad\qquad \text{(Eq. 8)}$$

Two conclusions should be emphasized here, which could only be confirmed by a parallel measurement with measuring rims and dynamometer:

- A theoretical axle load at the rear axle can be calculated taking into account the static axle load shift during the test with knowing simple geometric relations and by weighing the static axle load distribution.
- A net traction force can be calculated from the drawbar pull measured on the dynamometer, considering the rolling resistance force of the front wheels (measured or determined with an estimated rolling resistance ratio).

Figure 4 examines the repeatability of a test under identical conditions. Here, the curve already shows the net traction ratio κ over the slip σ which is the sum of the net traction force on both rear wheels in relation to the axle load. Since the actual values of κ are not in the focus here, the course is related to κ_{max}. The measuring configuration from the investigation above is kept. The slight variation of the five measurements among each other is relativized when the mean value is calculated. The course of the mean value does not change significantly with more than three measurements, which is why this is assumed to be a sufficient number of repetitions for the experiments.
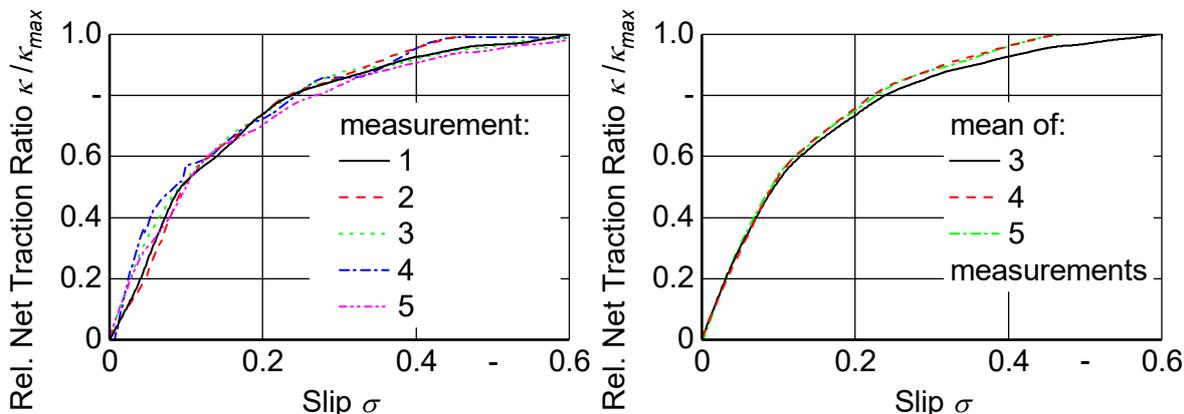
Figure 4: Repeatability of a test

Figure 5 shows a comparison between the net traction ratio of both rear wheels and the course of the net traction ratio calculated from the measurement results of the dynamometer. Both show good correlations over the whole slip range. This is compared with the results from the simulation for identical boundary conditions. The significant deviation at a slip of approx. 10–20%, which corresponds to typical operating condition during heavy field work, underlines the so far insufficient behaviour of the tyre-soil model. The maximum driving force coefficient in the simulation diverges by approx. 25% from the measurement, although this range is no longer relevant for practical use. The deviations are considered to be so significant that it is necessary to adjust the regression equations for a correction of the tyre-soil model.
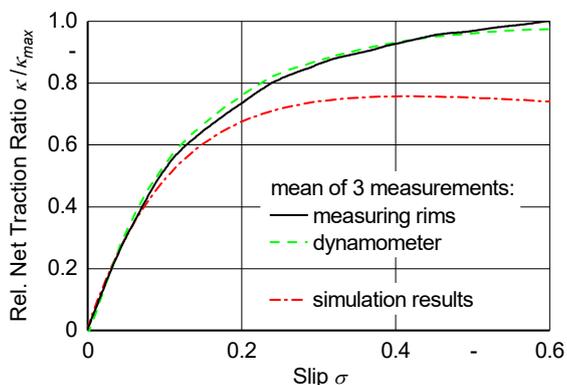

Figure 5: Comparison of net traction ratio between measurement and simulation

Using the tyre size 520/70 R 38 as an example, it can be shown that the measurement of the drawbar pull is sufficient to calculate the course of the net traction ratio for a specific tyre size if other boundary parameters are known which can be easily determined. For this purpose, certain assumptions for e.g. the rolling resistance force of the front wheels must be made and affect the reliability of the measurement results to a small extent. In contrast to the single wheel tester, measuring with a dynamometer has the advantage that it can be attached to any tractor. This allows a wide range of tyre dimensions to be examined flexibly under a huge variety of operating conditions.

Measurements and results

For the correction of the tyre-soil model, the tyre sizes required for the investigation are defined in Table 1. After the measuring methodology has been verified, the curves can be measured on tractors with matching tyre sizes. The tyres of the different tractors tested are all standard radial tyres. Since the simulation model is based on the assumption that the net traction ratio is independent of the wheel load within realistic limits, this variable was not investigated further. By measuring the tyre mounted to the tractor, the tyre load represents a realistic application for methodological reasons. The measurements also took place in the soil bin prepared as described above in June 2018 under dry soil conditions. For each tyre size according to Table 2, the tyre inflation pressure was varied from 0.8 bar to 2.0 bar. For each configuration 3 measurements were recorded.

Table 2: Paramaters of the investigated tyres

Tyre size	Wheel load in kg	Dynamic rolling radius r_{dyn} in m
520/70 R 38	2528	0.847
600/65 R 38	2300	0.832
650/65 R 38	2685	0.868
710/70 R 42	3410	0.983

Figure 6 shows an excerpt from the measuring results. Each curve contains the mean value of three repetitions. Following a steep incline the net traction ratio decreases by $\sigma \approx 0.1–0.15$ in all curves, but does not reach a threshold. Until the end of the measuring range, the curve is almost linear. The expected bend after reaching a local maximum due to a shearing of the upper soil layer, as it is included in the previous tyre-soil model, does not occur. The characteristic effects of tyre size and inflation pressure are clearly visible. Since diameter and width increase simultaneously, no distinction can be made between both influences. With the exception of the lowest tyre inflation pressure, a larger tyre generally shows a steeper increase, can therefore build up net traction force more quickly when the requirement of drawbar pull increases and achieves higher net traction ratios than smaller tyres at the same slip level. The influence of an increasing tyre inflation pressure is qualitatively sim-
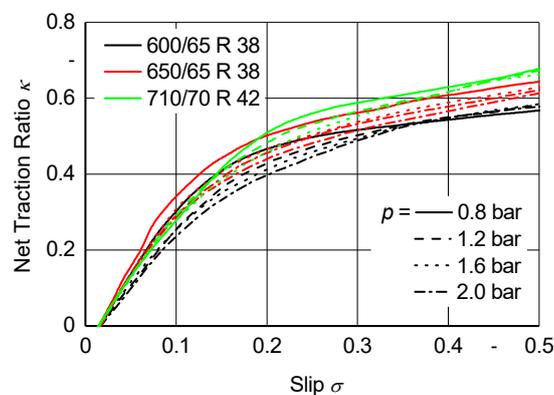

Figure 6: Measured net traction ratio/slip-curves

ilar for every tyre size. The increase in net traction force is greater and higher maximum values are reached. For the pressure p = 0.8 bar, all tyres show a slightly over-proportional reaction.

During the measurements, it can be observed that higher slip of the measuring vehicle above approx. 50 % leads to an exposure of firmer subsoil in the lower soil layer. Increased traction can be detected on this surface. The lack of a reduction in driving force at higher slip values is explained by this, but cannot be compensated with this measuring methodology and must be corrected during the processing of data.

Three major changes in the traction behaviour of current tyres compared to the behaviour of the model can be summarized as follows:

- The maximum net traction ratio that can be achieved is more closely dependent on the tyre size than previously shown.
- At the same time, the maximum net traction ratio tends to be reached at higher slip values.
- The influence of the tyre inflation pressure on the incline of the net traction ratio at low slip is higher for modern tyres.

Derivation of correction factors and simulation results

In order to adapt the regression model to the deviations in the traction behaviour of current tyres as summarized above, the introduction of correction factors is an appropriate method. Following the underlying approach of the tyre-soil model, a direct manipulation of the characteristic parameters of the net traction ratio/slip curves seems promising. The maximum net traction ratio must be taken more into account in dependency of the tyre dimension, as must the corresponding slip. The specific influence of the tyre inflation pressure on the characteristic curve has so far been underrepresented and must be extended. In Equations 9–11, the ideas are formulated mathematically using the additional correction factors β_1, β_2 and β_3.

$$\kappa_{max} = 0.31 + 0.13 k_{cover} + 0.11 k_{strength,A} + 0.09 k_{strength,B} + 0.07 k_{clay} \qquad \text{(Eq. 9)}$$

$$+ 0{,}09(-4 k_{moisture}^2 + 4 k_{moisture}) + \beta_1 k_{tyre}$$

$$\sigma_{\kappa,max} = \frac{-18 k_{cover} - 12 k_{strength,A} - 8 k_{strength,B} - 6 k_{clay} + 8 k_{moisture} + \beta_2}{100} \qquad \text{(Eq. 10)}$$

$$\kappa'(0) = 5 + 2{,}8 k_{cover} + 1{,}3 k_{strength,A} + \beta_3 k_{pressure} \qquad \text{(Eq. 11)}$$

The correction factors are determined empirically, for which further data available at the institute from previous measurements could be used. A post-processing of the measured net traction ratio/slip curves is necessary in advance. An idealization using the mathematical description according to Equation 1 allows the characteristic behaviour to be included subsequently. The least squares method is used for the equalization calculus. In Figure 7, the idealized curve shows, in contrast to the measurement, the decrease in the net traction ratio, which occurs beginning at $\sigma \approx 0.5$ in this example. The simulation result with the original tyre-soil model shows once again that the maximum net traction ratio from the measurement is not reached. With the idealized and the simulated curve as data input,

an equalization calculus is done according to the least squares method using all available data sets to determine the correction factors β_1, β_2 and β_3. The values in Table 3 result.

Table 3: Correction factors

Factor	Value
β_1	0.2204
β_2	62.5
β_3	−1.8233

Taking the factors into account, Figure 7 also shows the net traction ratio/slip curve simulated with the new model. The correlation with the idealized curve is better at lower slip than with the old model. In addition, the maximum net traction ratio is converged significantly better. The conclusion is underlined by the coefficient of determination, which is significantly higher with the new model.
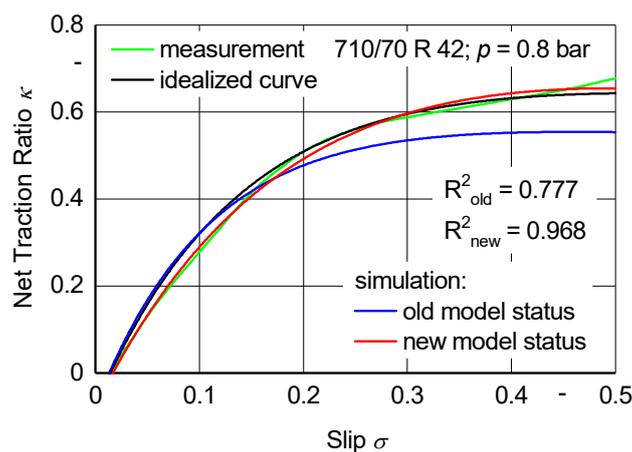

Figure 7: Procedure for test evaluation

Figure 8 shows an exemplary parameter variation of the tyre inflation pressure for the tyre 710/75 R 42. The factor β_3 now directly influences the incline at zero slip with the k-factor for the tyre inflation pressure. Likewise, the modified factor β_1 shapes the maximum of the curve more strongly with the now included influence of the tyre inflation pressure in k_{tyre}. At a net traction ratio of $\kappa = 0.4$, which is to be targeted for heavy field work (e.g. primary soil tillage), the slip can be reduced by more than 30 % when lowering the tyre inflation pressure from 2.0 bar to 0.6 bar. At the same time, the maximum net traction ratio is approx. 10 % higher due to reduced tyre inflation pressure. The influence is also significant with lower net traction ratios.
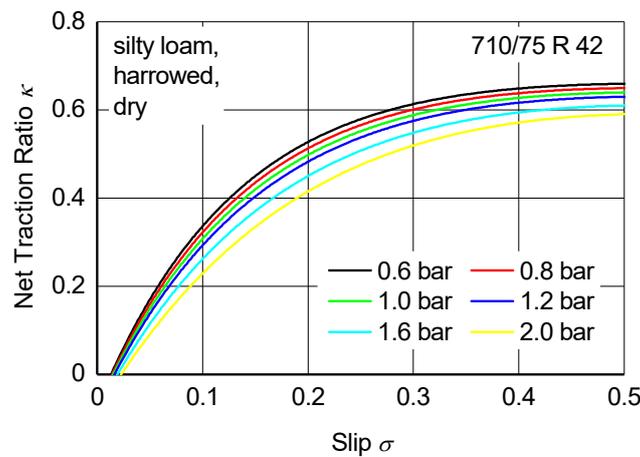
Figure 8: Influence of the tyre inflation pressure when considering the new correction factors

For a standard tractor in the power class 216–250 kW, the simulated net traction ratio/slip curves for front and rear wheel for typical operating scenarios are shown in Figure 9 for a tyre inflation pressure of 1.2 bar. The tyre size at the rear wheel is currently the largest standard tyre to be mapped with the model. When extrapolating to other soil conditions, the calculation shows a plausible behaviour for the influence of the different grounds.
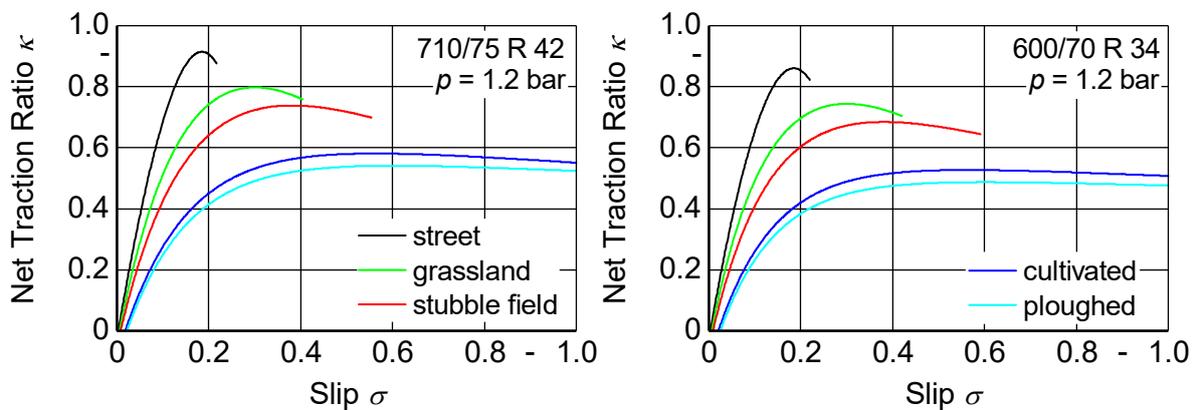

Figure 9: Simulated net traction ratio/slip curves for front and rear wheel of a standard 233 kW tractor in various soil conditions

Conclusions

Overall, the dependencies presented here can only be mapped to this extent with the new tyre-soil model. With the introduction of correction factors, a way was shown to generally adapt the model to a changed database. By determining the factors for the measured net traction ratio/slip curves presented, the applicability was extended towards larger tyre dimensions. The changes in traction behaviour of modern tyres since the measurements by STEINKAMPF (1986) at the end of the 1980s can now be described effectively. The HMM thus has a tyre-soil model for standard tractors up to 300 kW in which the tyre-side influences are updated and the soil-side influences are verified. Thus, the studies on fuel consumption in agricultural process chains within the EcoTech project correctly include the efficiency-influencing tyre-soil interaction.

References

Armbruster, K. (1991): Untersuchung der Kräfte an schräglaufenden angetriebenen Ackerschlepperrädern. Dissertation, Universität Stuttgart, 1991, Düsseldorf, VDI-Verlag

Bundesministerium für Umwelt, Naturschutz, Bau und Reaktorsicherheit (Hg.) (2018): Klimaschutz in Zahlen. Fakten, Trends und Impulse deutscher Klimapolitik, Berlin, BMUB

Bürger, A.; Böttinger, S. (2017): Quantifizierte Validierung des Hohenheimer Reifenmodells für fahrdynamische Untersuchungen. Landtechnik 72(6), S. 280–292, https://doi.org/10.15150/lt.2017.3173

Decker, M.; Frerichs, L. (2017): Effiziente Kraftstoffnutzung in der AgrarTechnik - EKoTech. In: Jahrbuch Agrartechnik 2016, Hg. Frerichs, L., Braunschweig, Institut für mobile Maschinen und Nutzfahrzeuge, S. 22–29

Europäische Kommission (2014): Mitteilung der Kommission an das Europäische Parlament, den Rat, den Europäischen Wirtschafts- und Sozialausschuss und den Ausschuss der Regionen - Ein Rahmen für die Klima- und Energiepolitik im Zeitraum 2020-2030. Pressemitteilung, Brüssel (Belgien)

Europäischer Rat (2014): Schlussfolgerungen vom 23. und 24. Oktober 2014, EUCO 169/14

Europäisches Parlament und Rat der Europäischen Union (2009): Verordnung (EU) Nr. 443/2009 des Europäischen Parlaments und des Rates vom 11. März 2014 zur Festsetzung von Emissionsnormen für neue Personenkraftwagen im Rahmen des Gesamtkonzepts der Gemeinschaft zur Verringerung der CO_2 -Emissionen von Personenkraftwagen und leichten Nutzfahrzeugen. Amtsblatt der Europäischen Union (L 103/15)

Europäisches Parlament und Rat der Europäischen Union (2014): Verordnung (EU) Nr. 333/2014 des Europäischen Parlaments und des Rates vom 11. März 2014 zur Änderung der Verordnung (EG) Nr. 443/2009 hinsichtlich der Festlegung der Modalitäten für das Erreichen des Ziels für 2020 zur Verringerung der CO_2 -Emissionen neuer Personenkraftwagen. Amtsblatt der Europäischen Union (L 103/15)

Fleck, B.; Nacke, E.; Böttinger, S.; Frerichs, L.; Hanke, S. (2014): Der Weg zur freiwilligen Selbstverpflichtung der europäischen Landtechnikindustrie zur Reduktion von CO2-Emissionen. In: VDI-MEG Tagung Landtechnik, 19./20.11.2014, Berlin, VDI Verlag, S. 301–308

KTBL (Hg.) (2016): Betriebsplanung Landwirtschaft 2016/17 - Daten für die Betriebsplanung in der Landwirtschaft. Darmstadt, 25. Aufl.

Kutzbach, H.D.; Bürger, A.; Böttinger, S. (2019): Rolling radii and moment arm of the wheel load for pneumatic tyres. Journal of Terramechanics 82, S. 13–21, https://doi.org/10.1016/j.jterra.2018.11.002

Meiners, A.; Böttinger, S. (2018): Leistungsbedarf und Leistungsverteilung im Mähdrescher - Untersuchung zukünftiger Einsparpotentiale im realen und virtuellen Versuch. In: Land.Technik 2018, 20.-21.11., Leinfelden, VDI Verlag, S. 149–157

Meiners, A.; Häberle, S.; Böttinger, S. (2017): Advancement of the Hohenheim Tractor Model – Adaption on current demands. In: VDI-MEG Tagung Landtechnik, 10./11.11.2017, Hannover, VDI Verlag, S. 245–253

Schreiber, M. (2006): Kraftstoffverbrauch beim Einsatz von Ackerschleppern im besonderen Hinblick auf CO2-Emissionen. Dissertation, Universität Hohenheim, 2006, Aachen, Shaker

Schreiber, M.; Kutzbach, H.D. (2008): Influence of soil and tire parameters on traction. Research in Agricultural Engeneering 54(2), S. 43–49

Schulze Zumkley, H. (2017): Reifenparameterermittlung aus Fahrversuchen mit einem Ackerschlepper unter besonderer Berücksichtigung des Hohenheimer Reifenmodells. Dissertation, Universität Stuttgart, 2016, Aachen, Shaker

Steinkampf, H. (1986): Betriebseigenschaften von Ackerschlepperreifen bei unterschiedlichen Einsatzbedingungen. Landbauforschung Völkenrode (Sonderheft 80), S. 2–37

Winkler, B.; Frisch, J. (2014): Weiterentwicklung der Zeitgliederung für landwirtschaftliche Arbeiten. In: 19. Arbeitswissenschaftliches Kolloquium des VDI-MEG Arbeitskreis Arbeitswissenschaften im Landbau, 11./12.03.2014, Dresden, S. 14–21

Zoz, F.M.; Grisso, R.D. (2003): Traction and Tractor Performance. ASAE Distinguished Lecture Series, Tractor Design

Authors

M. Sc. Arwid Meiners is research associate and **Prof. Dr.-Ing. Stefan Böttinger** is head of the Department of Fundamentals of Agricultural Engineering at the Institute of Agricultural Engineering at the University of Hohenheim, Garbenstr. 9, 70599 Stuttgart. E-mail: Arwid.Meiners@uni-hohenheim.de

Ing. Nicolò Regazzi was guest researcher at the University of Hohenheim and is research associate at the Department of Agriculture and Food Science at the University of Bologna, Viale Fanin 50, 40127 Bologna, Italy.

Acknowledgements